

Luminescence properties of Ce^{3+} ions in strontium bromoborate

Vladimir Dotsenko

A.V. Bogatsky Physico-Chemical Institute, Ukrainian Academy of Sciences,
86 Lustdorfskaya doroga 65080 Odessa, Ukraine. E-mail: physchem@paco.net

Received 13th August 1999, Accepted 26th October 1999

The luminescence properties of Ce^{3+} ions in strontium bromoborate are reported and discussed. In $\text{Sr}_{2(1-x)}\text{Ce}_{2x}\text{B}_5\text{O}_9\text{Br}$ ($x \leq 0.01$) solid solutions two principal Ce^{3+} centers are observed. The dominant center was found to be produced by the direct substitution of the dopant ion for Sr^{2+} without a local charge compensation. Upon UV excitation this center gives an intense emission with maxima at 326 and 349 nm. The other center is ascribed to an associate of a Ce^{3+} ion and a cation vacancy. It causes a broad band emission with a maximum at *ca.* 375 nm. The charge compensation mechanism on the cation sublattice includes the formation of one vacancy per two Ce^{3+} ions incorporated. $\text{Sr}_2\text{B}_5\text{O}_9\text{Br}:\text{Ce}^{3+}$ has potential for use as a storage phosphor for thermal-neutron detection, because of its favorable chemical composition and promising luminescent properties.

Introduction

The luminescence properties of Eu^{2+} ions in alkaline earth haloborates of the general formula $\text{M}_2\text{B}_5\text{O}_9\text{R}$ ($\text{M} = \text{Ca}, \text{Sr}, \text{Ba}$; $\text{R} = \text{Cl}, \text{Br}$) have been studied by Peters and Baglio,¹ Machida *et al.*² and Meijerink and Blasse.³ It has been shown that the Eu^{2+} -doped haloborates are efficient photoluminescent materials. Recently, materials of composition $\text{M}_2\text{B}_5\text{O}_9\text{Br}:\text{Eu}^{2+}$ ($\text{M} = \text{Ba}, \text{Sr}$) have been presented as promising storage phosphors for X-ray imaging⁴ and thermal-neutron detection.⁵ The results obtained on their photostimulated luminescence are consistent with a model in which halide vacancies act as electron traps and Eu^{2+} is involved in the hole trapping.

Here, we report on the luminescence of Ce^{3+} ions in strontium bromoborate $\text{Sr}_2\text{B}_5\text{O}_9\text{Br}$. The luminescent properties of Ce^{3+} in alkaline earth haloborates are interesting for several reasons. First, depending on the crystal field at the ion site, the decay time of Ce^{3+} emission varies between 20 and 80 ns, whereas the decay time of Eu^{2+} emission is typically 1 μs . Since the decay time of Ce^{3+} emission is shorter than that of Eu^{2+} emission, a screen containing Ce^{3+} -doped phosphor can be read faster, enabling high-speed imaging. Secondly, the mechanism of charge trapping has not been fully elucidated for $\text{M}_2\text{B}_5\text{O}_9\text{Br}:\text{Eu}^{2+}$, but the coexistence of Eu^{2+} and Eu^{3+} centers has been detected in $\text{M}_2\text{B}_5\text{O}_9\text{Br}:\text{Eu}^{2+}$ powder phosphors prepared in a neutral (N_2 , Ar) or a slightly reducing (H_2 - N_2) atmosphere.⁴⁻⁶ Also, one can expect that both Eu^{2+} and Eu^{3+} ions are essential in the trapping processes. The substitution of a trivalent ion for an alkaline earth ion requires the presence of a charge compensator to maintain the overall charge neutrality of the crystal. The Ce^{3+} ion has a very simple electron configuration in the ground and excited states: $4f^1$ and $5d^1$, respectively. Its emission is due to a fully allowed transition from the lowest crystal-field component of the $5d^1$ state to the ground state. In view of this, Ce^{3+} seems to be a suitable ion for study of the charge compensation mechanism for trivalent cations.

The crystal structure of $\text{Sr}_2\text{B}_5\text{O}_9\text{Br}$ consists of a three-dimensional $(\text{B}_5\text{O}_9)_\infty$ network, in which B_5O_{12} groups of three BO_4 tetrahedra and two BO_3 triangles are linked together.^{2,7} The strontium ions are surrounded by seven oxygen ions and two bromine ions. The average Sr–O and Sr–Br distances are 2.7 and 3.0 Å, respectively.

Experimental

$\text{Sr}_{2(1-x)}\text{Ce}_{2x}\text{B}_5\text{O}_9\text{Br}$ ($x = 0.0005$ – 0.03) solid solutions were prepared using a standard solid state method. Starting mixtures of SrCO_3 , $\text{SrBr}_2 \cdot n\text{H}_2\text{O}$ (10% excess), $\text{Ce}(\text{NO}_3)_3$ and H_3BO_3 (15% excess) were fired at a temperature of *ca.* 400 °C for 1 h and then at 750–800 °C for 3 h in a nitrogen stream. The samples were cooled, mortared to insure homogeneity and fired again at 800 °C for 2 h in a weakly-reducing atmosphere consisting of a nitrogen–hydrogen mixture containing 2% by volume of hydrogen. In some cases the starting powders were codoped with either alkali (Na^+ , K^+) or rare earth (Gd^{3+} , Sm^{3+}) ions. The sample of composition $\text{Sr}_{2(1-x)}\text{Ce}_{2x}\text{B}_5\text{O}_9\text{Cl}$ ($x = 0.0005$) was prepared in the same manner. All samples were checked by X-ray diffraction (XRD) using $\text{Cu-K}\alpha$ radiation. No impurity phases were detected in the XRD patterns. The emission and excitation spectra were recorded between 80 and 300 K using a LOMO SDL 1 spectrofluorometer equipped with a xenon lamp. The spectra were corrected for the photomultiplier sensitivity and the monochromator efficiency using a calibrated light source. For the decay time measurements, a flash xenon lamp and a pulsed YAG: Nd^{3+} laser ($\lambda_{\text{exc}} = 266$ nm) were employed. The measurements of excitation spectra at wavelengths shorter than 240 nm were performed at room temperature using synchrotron radiation at HASYLAB (Hamburg, Germany). These spectra were corrected for the wavelength dependent excitation intensity with the use of sodium salicylate as a standard.

Results and discussion

The vacuum-ultraviolet (V)UV excitation spectrum for $\text{Sr}_{1.98}\text{Ce}_{0.02}\text{B}_5\text{O}_9\text{Br}$ at 300 K shown in Fig. 1 consists of two regions. The excitation bands in the 200–310 nm region are attributed to transitions to the components of the Ce^{3+} 5d configuration which is split owing to the crystal field. Excitation of the host lattice starts at about 175 nm. It is seen that there is a sharp increase of the emission intensity between 175 and 80 nm. Most probably, a shoulder at *ca.* 75 nm is caused by the small penetration depth of the radiation leading to energy loss processes. It is known that the concentration of defects near the surface is higher than in the volume and this can cause a change of luminescence efficiency with wavelength and penetration depth. It should be

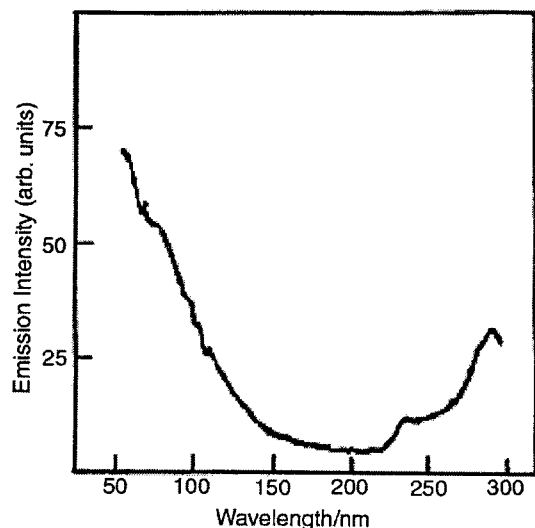


Fig. 1 (V)UV excitation spectrum of $\text{Sr}_{1.98}\text{Ce}_{0.02}\text{B}_5\text{O}_9\text{Br}$ monitoring the $5d \rightarrow 4f$ emission of Ce^{3+} ($\lambda_{\text{em}} = 355 \text{ nm}$) at 300 K.

noted that in the 50–175 nm region, the shape of the excitation spectrum is very similar to that of $\text{Sr}_2\text{B}_5\text{O}_9\text{Br}$ doped with both Sm^{2+} and Eu^{2+} .⁸ The question arises as to what kind of transitions can be responsible for the main features of the VUV excitation spectrum. In this connection, we point out that in the excitation spectra of Eu^{3+} in $\text{Sr}_2\text{B}_5\text{O}_9\text{Br}$ a broad band appears that peaks at λ_{max} ca. 215 nm ($46\,510 \text{ cm}^{-1}$).⁵ Similar features have been found in the absorption and excitation spectra of many materials doped with europium. These bands result from charge transfer (CT) transitions of Eu^{3+} –ligand complexes. For $\text{Sr}_2\text{B}_5\text{O}_9\text{Br}:\text{Eu}^{3+}$, it may be questioned whether the bromine or oxygen ligands are involved in the CT. The spectral position of the charge transfer band is determined by the oxidizing character of the central metal ion and by the properties of the set of ligands. It is well known⁹ that the position of this absorption band tends to shift to lower energies from oxides to chlorides to bromides. It is interesting to compare the λ_{max} values found for lanthanum orthoborate LaBO_3 ($37\,700 \text{ cm}^{-1}$),¹⁰ lanthanum oxyhalides LaOX ($X = \text{Cl}, \text{Br}$) ($33\,300\text{--}30\,700 \text{ cm}^{-1}$)¹¹ and $\text{La}_3\text{TaO}_4\text{Cl}_6$ ($31\,750 \text{ cm}^{-1}$).¹² It should be noted that in LaOX ($X = \text{Cl}, \text{Br}$) and $\text{La}_3\text{TaO}_4\text{Cl}_6$, the La ions have the same coordination number, $N=9$, as in LaBO_3 , however, the anion environment around La ion comprises four and seven halogen ions, respectively. In terms of our work it is significant that the maximum of the CT band for $\text{Sr}_4\text{O}_7:\text{Eu}^{3+}$ is located at 210 nm ($47\,600 \text{ cm}^{-1}$)¹³ a value comparable with that found for $\text{Sr}_2\text{B}_5\text{O}_9\text{Br}:\text{Eu}^{3+}$. Since in Sr_4O_7 the cation has a nine-fold coordination, one can expect that for $\text{Sr}_2\text{B}_5\text{O}_9\text{Br}:\text{Eu}^{3+}$, the ligand to europium CT takes place from the highest filled molecular orbital which is localized mainly on the oxygen and to a lesser extent also on the bromine. This implies that the electronic structure of $\text{Sr}_2\text{B}_5\text{O}_9\text{Br}$ is mainly determined by the borate groups. Taking into account the results of electronic structure calculations on rare earth orthoborates¹⁴ and magnesium fluoroborates,¹⁵ we believe that the top of the valence band of $\text{Sr}_2\text{B}_5\text{O}_9\text{Br}$ arises from 2p oxygen states. Transitions from these states to vacant 2s and 2p boron states cause the dominant features of the VUV excitation spectrum. Note that the position of the 2p $\text{O} \rightarrow 2s \text{ B}$ and 2p $\text{O} \rightarrow 2p \text{ B}$ transitions is largely independent of the rare earth ion present but is affected by the type of borate group. Assuming a direct band-gap model, the band-gap energy (E_g) of $\text{Sr}_2\text{B}_5\text{O}_9\text{Br}$ was estimated to be 7.1 eV. This value is comparable with those for other borates, e.g. $\beta\text{-BaB}_2\text{O}_4$ (6.4 eV),¹⁶ YBO_3 and ScBO_3 (ca. 7.0 eV).¹⁷

Fig. 2 shows the changes of the emission and UV excitation

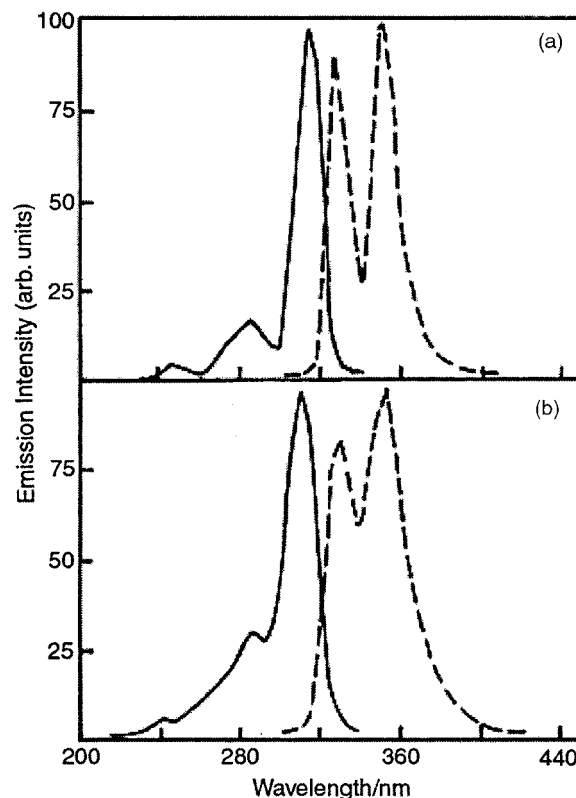


Fig. 2 Emission and excitation spectra of $\text{Sr}_{2(1-x)}\text{Ce}_x\text{B}_5\text{O}_9\text{Br}$ solid solutions at 100 K; (a) $x=0.0005$, (b) $x=0.0003$. The emission spectra were recorded upon excitation at 290 nm. The excitation spectra were recorded for emission at 370 nm.

spectra of the $\text{Sr}_{2(1-x)}\text{Ce}_x\text{B}_5\text{O}_9\text{Br}$ solid solutions with increasing cerium concentration. In the emission spectrum of the sample with $x=0.0005$ a broad band with two maxima is observed. At 100 K the maxima are located at 326 and 349 nm. The energy gap between the maxima is in agreement with the spin–orbit splitting of the Ce^{3+} ground state, which amounts to ca. 2000 cm^{-1} . With increasing temperature, the emission band shifts somewhat towards longer wavelengths. In the excitation spectrum of this emission several bands in the 240–320 nm region are observed. The lowest excitation band is situated at 314 nm, so that the Stokes shift of the emission is small (ca. 1800 cm^{-1}). Upon direct excitation of the Ce^{3+} ions in the 260–310 nm range the decay of the emission is single-exponential with a decay time of $29 \pm 2 \text{ ns}$. Note that the excitation and emission spectra of Ce^{3+} in $\text{Sr}_2\text{B}_5\text{O}_9\text{Cl}$ are very similar to those observed for $\text{Sr}_2\text{B}_5\text{O}_9\text{Br}$, however, the emission maxima are situated at 322 and 345 nm. The center of gravity of the crystal-field split 5d configuration is influenced by the host lattice anion. The weaker nephelauxetic effect of Cl^- in comparison with Br^- explains the shift to shorter wavelengths of the excitation and emission bands in the chloroborate compared to the bromoborate. The absolute quantum efficiency of the $\text{Sr}_2\text{B}_5\text{O}_9\text{Br}:\text{Ce}^{3+}$ emission was difficult to estimate. In view of the fact that the emission intensity of $\text{Sr}_{2(1-x)}\text{Ce}_x\text{B}_5\text{O}_9\text{Br}$ ($x=0.0005$) is temperature independent in the range 80–300 K, one can suppose that the quantum efficiency of the Ce^{3+} emission in $\text{Sr}_2\text{B}_5\text{O}_9\text{Br}$ is high. Note that high quantum efficiencies of Ce^{3+} emission were also reported in CaSO_4 ¹⁸ and CaF_2 .¹⁹

As can be seen from Fig. 2, increasing the Ce^{3+} concentration has a strong influence on the excitation and emission spectra. It is evident that the emission spectrum of the sample with $x=0.0003$ is a superposition of several bands. Fitting the spectrum to Gaussian functions indicates the presence of a broad emission band with a maximum at ca. 375 nm. In the excitation spectrum of this emission at least one extra band

with a maximum at 288 nm is observed. It was found that addition of Na^+ ions to the firing mixture for charge compensation reduces the relative intensity of the 375 nm emission band. Luminescence measurements were also carried out on $\text{Sr}_2\text{B}_5\text{O}_9\text{Br}:\text{Ce}^{3+}$, K^+ samples which gave spectra indistinguishable from those obtained for $\text{Sr}_2\text{B}_5\text{O}_9\text{Br}:\text{Ce}^{3+}$, Na^+ . The spectra of samples with $x \geq 0.01$ are more complex. The emission of the sample with $x = 0.01$ (Fig. 3) extends from 310 to 430 nm having a maximum at *ca.* 353 nm and a shoulder at *ca.* 335 nm. In the excitation spectrum of the 335 nm emission a broad band with a maximum at *ca.* 300 nm is present. Codoping with either rare earth ions or alkali ions had drastic effects on the relative intensities of bands in the spectra. Normalized emission spectra at 100 K of the samples codoped with both Ce^{3+} and either Gd^{3+} or Na^+ are shown in Fig. 3. It can be seen that codoping with Na^+ produces a spectrum in which the emission band with maxima at 326 and 349 nm dominates. Codoping with Gd^{3+} (as well as an increase of cerium concentration) broadens the Ce^{3+} -emission bands. Also, in the presence of Gd^{3+} , an additional line appears in the emission spectrum at 313 nm. This line corresponds to the ${}^6\text{P}_{7/2} \rightarrow {}^8\text{S}_{7/2}$ transition in Gd^{3+} ions.

Upon excitation by either UV light or ionizing radiation the observed decay curves of the $5d \rightarrow 4f$ emission of $\text{Sr}_{2(1-x)}\text{Ce}_{2x}\text{B}_5\text{O}_9\text{Br}$ ($x \geq 0.001$) solid solutions depend on emission wavelength. It is clear that this is a consequence of the existence of several different Ce^{3+} sites. The decay curves of the emission of $\text{Sr}_{1.98}\text{Ce}_{0.02}\text{B}_5\text{O}_9\text{Br}$ excited with $\lambda_{\text{exc}} = 280$ nm for two different emission wavelengths are shown in Fig. 4. The decay curve of the emission at 355 nm shows a strong deviation from exponential behaviour. This is due to energy transfer between the different centers and overlap of their emission spectra. The decay of the emission at 390 nm is non-exponential for short times after the excitation pulse, but exponential for longer times. The exponential part can be characterized by a time constant of 38 ± 3 ns. Upon excitation at $\lambda_{\text{exc}} = 114$ nm the decay [Fig. 4(c)] is seen to have a non-exponential time dependence. It is clear that its duration is much longer than the decay time of the excited level of the predominant cerium center. This slow decay is ascribed to relatively slow energy transfer processes terminating on the cerium ions.

Let us now discuss the spectra shown in Fig. 2. When cerium is incorporated into $\text{Sr}_2\text{B}_5\text{O}_9\text{Br}$ as an impurity ion, it enters in a trivalent state and substitutes for a strontium ion. It is obvious to assume that the dominant center with emission maxima at 326 and 349 nm consists of a Ce^{3+} ion on an Sr^{2+} site without a nearby charge compensator. The weaker Ce^{3+} emission with

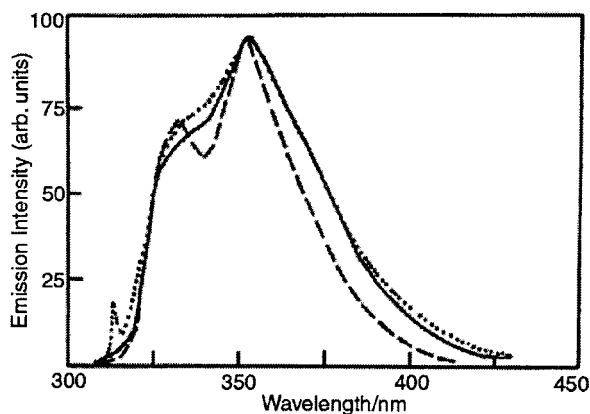


Fig. 3 Comparison of normalized emission spectra of $\text{Sr}_{1.98}\text{Ce}_{0.02}\text{B}_5\text{O}_9\text{Br}$ (—), $\text{Sr}_{1.96}\text{Ce}_{0.02}\text{Gd}_{0.02}\text{B}_5\text{O}_9\text{Br}$ (···) and $\text{Sr}_{1.96}\text{Ce}_{0.02}\text{Na}_{0.02}\text{B}_5\text{O}_9\text{Br}$ (---) at 100 K. The spectra were recorded upon excitation at 280 nm.

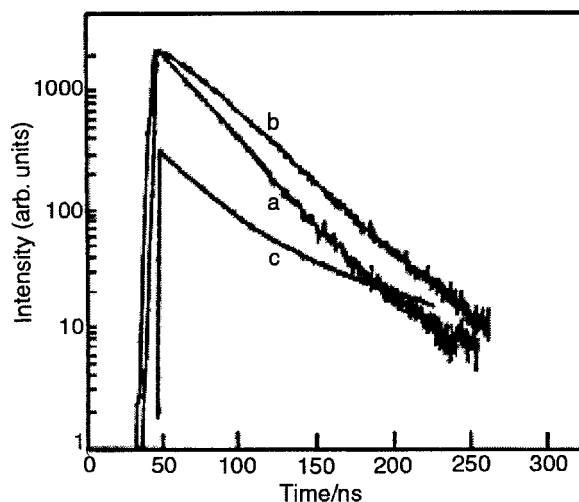


Fig. 4 Decay curves of the emission at 355 nm (a, c) and 390 nm (b) of $\text{Sr}_{1.98}\text{Ce}_{0.02}\text{B}_5\text{O}_9\text{Br}$ recorded upon excitation at 280 nm (a, b) and 114 nm (c). Measurements were performed at 300 K.

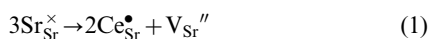
$\lambda_{\text{max}} = 375$ nm is ascribed to Ce^{3+} ions associated with a cation vacancy, *i.e.* $(\text{Ce}_{\text{Sr}}\text{V}_{\text{Sr}})'$. This assumption is based on the following facts:

(i) the relative intensity of this emission increases with increasing cerium concentration and decreases with the introduction of monovalent cations (Na^+ , K^+).

(ii) owing to the strengthening of the covalent bond between Ce^{3+} and its environment, the vacancy can be responsible for the lower-energy position of the 375 nm emission band in comparison with the single-ion emission band.

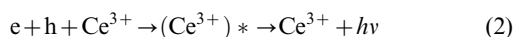
Another compensation mechanism expected for $\text{Sr}_2\text{B}_5\text{O}_9\text{Br}:\text{Ce}^{3+}$ is the replacement of the nearest neighbouring Sr^{2+} ions by monovalent impurity ions such as Na^+ and K^+ . The addition of Na^+ would be expected to inhibit the formation of Ce^{3+} -vacancy pairs $(\text{Ce}_{\text{Sr}}\text{V}_{\text{Sr}})'$ in favor of the more energetically stable $(\text{Ce}_{\text{Sr}}\text{Na}_{\text{Sr}})^{\times}$ centers. In comparison with the isolated ions, these centers usually give a broad emission at slightly lower energy. However, no significant changes caused by the appearance of $(\text{Ce}_{\text{Sr}}\text{Na}_{\text{Sr}})^{\times}$ -associates were detected in our experiments. This indicates that the influence of a monovalent cation on the surrounding of the Ce^{3+} ion is relatively weak. The explanation for this lies in the fact that the Sr^{2+} ions in $\text{Sr}_2\text{B}_5\text{O}_9\text{Br}$ are located alternately with Br^- ions in tunnels of the $(\text{B}_5\text{O}_9)_{\infty}$ network, and each Sr^{2+} ion is considerably isolated from neighbouring Sr^{2+} ions by the borate groups and Br^- ions. The Sr^{2+} ions in $\text{Sr}_2\text{B}_5\text{O}_9\text{Br}$ have four nearest Sr^{2+} neighbours at an average distance of 4.4 Å and four next-nearest neighbours at a distance of 5.6–5.8 Å.² These distances appear to be too large for a detectable influence of Na^+ and K^+ on the surrounding of the Ce^{3+} ion. Such a situation was reported for Eu^{3+} in $\text{CaSO}_4 \cdot 2\text{H}_2\text{O}$.²⁰ In this compound no influence of Na^+ on the luminescence spectra was observed. This was ascribed to the large distance between the Ca^{2+} ions in this structure, *viz.* 4.1 Å. The spectrum of the sample with $x = 0.01$ is complicated (Fig. 3). There is a distinct contribution from $\text{Ce}_{\text{Sr}}^{\bullet}$ and $(\text{Ce}_{\text{Sr}}\text{V}_{\text{Sr}})'$ centers in it, but besides this the spectrum is probably due to several Ce^{3+} centers with slightly different crystal field parameters. This can be viewed as a concentration effect, leading to the appearance of cerium centers directly surrounded by rare earth ions (Ce^{3+} , Gd^{3+}). Since rare earth ions can be located at several different distances from an emitting ion, the different local fields result in inhomogeneously broadened spectra. Note that because of their close proximity, these ions are coupled, so that energy can be transferred from one ion to another. Finally, the

introduction of Ce^{3+} ions in $Sr_2B_5O_9Br$ takes place in accordance with the scheme:



i.e. for every two Ce^{3+} ions there is one vacancy in the strontium sublattice. It is evident that there is a second possible scheme. It involves a substitution of an O^{2-} ion for a Br^- . Electron paramagnetic resonance measurements⁵ on $Sr_2B_5O_9Br:Eu^{2+}$ powder phosphors showed a radiation-induced signal which can be attributed to an oxygen center having a trapped hole. The results reported here indicate that while this mechanism can not be excluded, its role is of limited importance.

As noted above, excitation spectra show that the Ce^{3+} -luminescence is caused by optical excitation of an electron from the 4f ground state to levels of the 5d states or by ionizing an electron from the O 2p (Br 4s) valence band. In the latter case, one type of fast excitation process is free electron and hole capture:



The results of the decay time measurements (Fig. 4) show that under VUV excitation many free holes and electrons are trapped in the crystal before they can excite cerium ions. As far as the charge-uncompensated Ce_{Sr}^{\bullet} center is concerned, because of its positive effective charge, the free-hole capture rate is probably relatively small. On the other hand, electron capture may be delayed, requiring the thermal activation of electrons from traps such as anion vacancies. From the decay measurements presented, it is not possible to conclude which process is responsible for the trapped electrons and holes. For more information on this subject, additional experiments should be performed. The results of luminescence studies reported here can be useful in modeling the processes occurring in these materials during irradiation and subsequent photostimulation. For example, Meijerink and Blasse⁴ and Knitel *et al.*⁶ have observed a decrease of the Eu^{3+} emission intensity after X-ray irradiation of $M_2B_5O_9Br:Eu$ ($M = Sr, Ba$). Assuming that this is in part due to trapping processes, one can expect that X-ray irradiation of $M_2B_5O_9Br:Eu$ will preferentially reduce the concentration of Eu^{3+} ions which occupy M^{2+} sites without a local charge compensation, producing a more stable center. The other Eu^{3+} ions must be left predominantly in the trivalent state. Also, we feel that low-temperature measurements on single crystals could reveal other centers not clearly shown in our present studies.

Conclusion

In $Sr_{2(1-x)}Ce_{2x}B_5O_9Br$ ($x \leq 0.01$) solid solutions two principal Ce^{3+} centers are observed. The dominant center was found to be produced by the direct substitution of the dopant ion for Sr^{2+} without a local charge compensation. The other center is ascribed to an associate of a Ce^{3+} ion and a cation vacancy. The charge compensation mechanism on the cation sublattice

includes the formation of one vacancy per two Ce^{3+} ions incorporated.

The short decay time (30–40 ns) of the Ce^{3+} emission upon 4f→5d excitation provides a possibility for fast photostimulated luminescence. The decay of the luminescence upon VUV excitation is non-exponential and its duration is longer than the intrinsic Ce^{3+} 5d→4f decay time. This slow decay is attributed to action of relatively slow energy transfer processes terminating on the cerium ions. Finally, the luminescence properties of $Sr_{2(1-x)}Ce_{2x}B_5O_9Br$ solid solutions are promising enough to investigate their storage properties in the future.

Acknowledgements

The author is grateful to Dr A. Voloshonovskii for performing the experiments at the synchrotron of Hamburg (Germany) and Dr I. Berezovskaya for her assistance in the preparation of the samples and for fruitful discussions.

References

- 1 T. E. Peters and J. Baglio, *J. Inorg. Nucl. Chem.*, 1971, **32**, 1089.
- 2 K. Machida, G. Adachi, N. Yasuoka, N. Kasai and J. Shiohara, *Inorg. Chem.*, 1980, **19**, 3807.
- 3 A. Meijerink and G. Blasse, *J. Lumin.*, 1989, **43**, 283.
- 4 A. Meijerink and G. Blasse, *J. Phys. D: Appl. Phys.*, 1991, **24**, 626.
- 5 M. Knitel, *New Inorganic Scintillators and Storage Phosphors for Detection of Thermal Neutrons*, PhD Thesis, Delft University, 1998.
- 6 M. J. Knitel, P. Dorenbos, J. Andriassen, C. W. E. Van Eijk, I. Berezovskaya and V. Dotsenko, *Radiat. Meas.*, 1998, **29**, 327.
- 7 C. Fouassier, A. Lavoisier and P. Hagenmuller, *J. Solid State Chem.*, 1971, **3**, 206.
- 8 V. P. Dotsenko, V. N. Radionov and A. S. Voloshinovskii, *Mater. Chem. Phys.*, 1998, **57**, 134.
- 9 R. Reisfeld and C. K. Jorgensen, *Lasers and Excited States of Rare Earths*, Springer-Verlag, Berlin–Heidelberg–New York, 1977.
- 10 A. Bril and W. L. Wanmaker, *J. Electrochem. Soc.*, 1964, **111**, 1363.
- 11 G. Blasse and A. Bril, *J. Chem. Phys.*, 1967, **46**, 2579.
- 12 J. W. Severin, M. J. J. Lammers, G. Blasse, L. H. Brixner and C. C. Torardi, *J. Solid State Chem.*, 1987, **66**, 318.
- 13 J. W. M. Verwey, G. J. Dirksen and G. Blasse, *J. Phys. Chem. Solids*, 1992, **53**, 367.
- 14 M. V. Ryzhkov, V. P. Dotsenko, N. P. Efrushina and V. A. Gubanov, *Zhur. Struk. Khim.*, 1991, **32**, 26.
- 15 M. V. Ryzhkov, V. P. Dotsenko, N. P. Efrushina and V. A. Gubanov, *Opt. Spectrosc.*, 1991, **70**, 271.
- 16 R. H. French, J. W. Ling, F. S. Ohuchi and C. T. Chen, *Phys. Rev. B: Condens. Matter*, 1991, **44**, 8496.
- 17 J. Koike, T. Kojima, R. Toyonaga, A. Kagami, T. Hase and I. Shuji, *J. Electrochem. Soc.*, 1979, **126**, 1008.
- 18 D. Van der Voort and G. Blasse, *J. Solid State Chem.*, 1990, **87**, 350.
- 19 L. J. Lyu and D. S. Hamilton, *J. Lumin.*, 1991, **48–49**, 251.
- 20 D. Van der Voort, G. Blasse, G. Witkamp, G. M. Van Rosmalen and L. H. Brixner, *Mater. Chem. Phys.*, 1989, **24**, 175.

Paper a906584i